Developments in Mathematical Algorithms and Computational Tools for Proton CT and Particle Therapy Treatment Planning

Yair Censor, Keith E. Schubert, *Senior Member, IEEE,* and Reinhard W. Schulte, *Member, IEEE*.
Preprint accepted for publication in IEEE Transactions on Radiation and Plasma Medical Sciences.
August 16, 2021.

***Abstract*—We summarize recent results and ongoing activities in mathematical algorithms and computer science methods related to proton computed tomography (pCT) and intensity-modulated particle therapy (IMPT) treatment planning. Proton therapy necessitates a high level of delivery accuracy to exploit the selective targeting imparted by the Bragg peak. For this purpose, pCT utilizes the proton beam itself to create images. The technique works by sending a low-intensity beam of protons through the patient and measuring the position, direction, and energy loss of each exiting proton. The pCT technique allows reconstruction of the volumetric distribution of the relative stopping power (RSP) of the patient tissues for use in treatment planning and pre-treatment range verification. We have investigated new ways to make the reconstruction both efficient and accurate. Better accuracy of RSP also enables more robust inverse approaches to IMPT. For IMPT, we developed a framework for performing intensity-modulation of the proton pencil beams. We expect that these developments will lead to additional project work in the years to come, which requires a regular exchange between experts in the fields of mathematics, computer science, and medical physics. We have initiated such an exchange by organizing annual workshops on pCT and IMPT algorithm and technology developments. This report is, admittedly, tilted toward our interdisciplinary work and methods. We offer a comprehensive overview of results, problems, and challenges in pCT and IMPT with the aim of making other scientists wanting to tackle such issues and to strengthen their interdisciplinary collaboration by bringing together cutting-edge know-how from medicine, computer science, physics, and mathematics to bear on medical physics problems at hand.**

***Index Terms*—proton therapy, proton computed tomography, intensity-modulated therapy, blob basis functions, superiorization, data partitioning, Monte Carlo simulation, digital phantoms, motion-adapted reconstruction**

I. Introduction

Proton therapy is becoming increasingly common for cancer radiation therapy. Protons afford tissue-sparing advantages that should be carefully tested against the best available photon therapy techniques, i.e., intensity-modulated radiation therapy (IMRT). However, this requires further development of image-guidance and inverse planning techniques for proton and ion therapy. This report summarizes some developments of advanced algorithmic and computational methods for proton computed tomography (pCT) and for intensity-modulated particle therapy (IMPT) that we developed by applying expertise in optimization algorithms, computer science, and medical physics, related to proton and ion therapy. We give references to published work when applicable and include details about work-in-progress. The purpose of over-viewing our work in this rapidly evolving field is to inspire other researchers to contribute to it in an interdisciplinary fashion.

Both IMPT and pCT are "inverse problems"; they are processes of calculating causal factors from a set of observations they produced. For example, in IMPT or IMRT the fluence of individual pencil beams or beamlets will produce a dose distribution and the clinical prescriptions play the role of "observations" in this framework from which the proper fluences are calculated. Likewise, in pCT, relative stopping power (RSP) is the property of tissues that results in energy loss of protons and ions. Here, measured energy loss of individual protons traversing the object are the "observations" and the RSP is calculated from these observations, forming the pCT image. Starting from this premise, we discuss the following topics mostly from the mathematical and computational points of view:

- The development of a feasibility-seeking approach and algorithms for treatment planning of IMPT.
- The superiorization methodology (SM) combined with the diagonally relaxed orthogonal projection (DROP) feasibility-seeking algorithm.
- The application of the SM to total variation superiorization (TVS) for pCT reconstruction.
- The use of blob basis functions and the reconstruction from pCT data acquired in the presence of organ motion.
- The derivative-free framework for the SM with component-wise perturbations.
- The selection of appropriate digital anthropomorphic phantoms for exploring pCT and IMPT.
- The selection of simulation tools to generate pCT data and, as a forward calculation method, to calculate dose contributions from proton pencil beams.
- The development of tools to compare pCT and IMPT results with those of concurrent methods.
- The development of code optimized for general purpose graphics processing units (GPGPU) that combines al-

Y. Censor is with the Department of Mathematics, The University of Haifa Haifa, Israel

K. E. Schubert is with the Department of Electrical and Computer Engineering, Baylor University, Waco, TX, USA

R. W. Schulte is with the Department of Basic Sciences, Loma Linda University Loma Linda, CA, USA

gorithmic advances, memory, and computational tuning, required to achieve speedup.
- The efforts to acquire pCT data with phantoms using the preclinical pCT scanner at the Northwestern Medicine Chicago Proton Center (NMCPC).

II. Model Formulations and Mathematical Algorithms for pCT and IMPT Inverse Problems

In this section, we give an overview of some of the methods used in the investigations of the topics listed above. If available, we point to additional details about the methods in the published literature. From the mathematical modeling and algorithmic points of view, we take recent algorithmic developments and "translate" them to applications in pCT and IMPT inverse problems. We demonstrate this approach by two specific novel techniques that were investigated and have been published but can benefit from further adaptation and refinement for these applications. These are the **superiorization methodology** for pCT image reconstruction and the **split inverse problem paradigm** for IMPT.

The core of the fully-discretized inverse problems of IMPT and pCT problems discussed here consists of the constraints, which are dictated by the underlying physical model. In the *feasibility approach*, we look at *convex feasibility problems* (CFPs) of the form: find a vector $x^* \in C := \cap_{i=1}^{I} C_i$, where the sets $C_i \subseteq R^J$ are nonempty closed convex subsets of the Euclidean space R^J, see, e.g., [1]–[3] or [4, Chapter 5] for results and references on this broad topic.

Both IMPT inverse planning and pCT, as well as other inverse problems where the underlying system has very large values of I and J and is often very sparse, fall under this category. Under these circumstances, *projection methods* are beneficial [1], [5]–[9]. These are iterative algorithms that use projections onto sets, e.g., hyperplanes or half-spaces in the linear cases, while relying on the general principle that when a family of, usually closed and convex, sets is present, projections onto the given individual sets are easier to perform than projections onto other sets (intersections, image sets under some transformation, etc.) that are derived from the given individual sets.[1]

A. The Superiorization Methodology

The superiorization methodology (SM) can be applied to the data of constrained minimization (CM) problems of the form: $\text{minimize}\,\{\phi(x) \mid x \in C\}$, where $\phi : R^J \to R$ is a target function, and $C \subseteq \Theta \subseteq R^J$ is a given feasible set defined by constraints, see, e.g., [18]. It aims at finding a feasible point that is superior (with respect to the target function value) to one returned by an algorithm that is only feasibility-seeking. In doing so, SM is situated between feasibility-seeking and full-fledged CM.

There are two main reasons why superiorization is beneficial: (i) for a problem for which an exact CM algorithm has not yet been discovered, but there are iterative feasibility-seeking methods that provide constraints-compatible solutions, which can be turned by the superiorization methodology into methods that will be practically useful for the target function reduction effort; and (ii) when existing exact optimization algorithms are either very time consuming or require too much computer space for large problems to be processed by run-of-the-mill computers. On the other hand, space- and time-efficient algorithms exist for constraints-compatibility-seeking, and these can be turned into efficient algorithms for superiorization. Examples of such situations are given in [19], [20].

There is no general answer yet to the question under which circumstances one should resort to superiorization as the method of choice. Even when tractable constrained optimization algorithms are available, the SM often yields better or comparable results. This has been demonstrated in [19] where a comparison between the projected subgradient method and SM showed that the SM performed better when applying it to an image reconstruction from projections problem. Many works cited on [21] attest to the practical success of the SM in a variety of situations.

In the SM, one associates with the feasible set C a proximity function $Prox_C : \Theta \to R_+$, which is an indicator of how incompatible a vector $x \in \Theta$ is with the constraints. For any given $\varepsilon > 0$, a point $x \in \Theta$ for which $Prox_C(x) \leq \varepsilon$ is called an *ε-compatible point* for C.

The ε-output of a sequence, defined in [22], can be explained as follows. For a nonnegative ε and a sequence $R := \left(x^k\right)_{k=0}^{\infty}$ of points in Θ, the ε-output of the sequence R is a point $x \in \Theta$ that has the following properties: $Prox_C(x) \leq \varepsilon$, and there is a nonnegative integer K such that $x^K = x$ and, for all nonnegative integers $k < K$, we have $Prox_C(x^k) > \varepsilon$. If there is such an x, then it is unique. If there is no such x, then we say that the ε-output of the sequence is *undefined* and otherwise, that it is *defined*.

In order to "superiorize" a feasibility-seeking algorithm, commonly called the "Basic Algorithm", represented by the iteration $x^{k+1} = \boldsymbol{A}_C(x^k)$, we need it to have *strong perturbation resilience* in the sense that for every $\varepsilon > 0$, for which an ε-output is defined for a sequence generated by the Basic Algorithm for every $x^0 \in \Theta$, we have also that the ε'-output is defined for every $\varepsilon' > \varepsilon$ and for every sequence $\left\{y^k\right\}_{k=0}^{\infty}$ generated by

$$y^0 = x^0, \;\; y^{k+1} = \boldsymbol{A}_C\left(y^k + \beta_k v^k\right), \text{ for all } k \geq 0, \qquad (1)$$

where the vector sequence $\left\{v^k\right\}_{k=0}^{\infty}$ is bounded and the scalars $\{\beta_k\}_{k=0}^{\infty}$ are such that $\beta_k \geq 0$, for all $k \geq 0$, and $\sum_{k=0}^{\infty} \beta_k < +\infty$. See, e.g., [19], [22] for additional details.

[1]The fully-discretized formulation of the inverse problem of IMRT treatment planning was not commonly accepted in the early days as it is today. In 1982, Brahme, Roos, and Lax tried to solve the inverse problem of radiation therapy treatment planning in its continuous (not fully-discretized) formulation via integral inversion [10]. However, to be able to generate the required inverse transform, they had to make unrealistic assumptions on the model that rendered their analysis impractical. Altschuler and Censor proposed in 1984 [11] a fully-discretized IMRT model. Here, "fully-discretized" means that not only the irradiated volume is discretized into voxels but that also the external radiation field is discretized into "rays" ("beamlets" or "pencil beams" in today's language). The initial conference report was followed by a sequence of papers that established this approach [12]–[14]. To the best of our knowledge, these and the independent 1990 paper of Bortfeld et al. [15] were the first publications that suggested the fully-discretized approach to the inverse problem of IMRT, see also [16] and the introduction of [17].

Algorithm 1: The Superiorized Version of the Basic Algorithm

set $k = 0$
set $y^k = y^0$
set $\ell = -1$
repeat
  set $n = 0$
  set $y^{k,n} = y^k$
  while $n<N$
    set $v^{k,n}$ to be a non-ascending vector for ϕ at $y^{k,n}$
    set *loop=true*
    while *loop*
      set $\ell = \ell + 1$
      set $\beta_{k,n} = \eta_\ell$
      set $z = y^{k,n} + \beta_{k,n} v^{k,n}$
      if $\phi(z) \leq \phi\left(y^k\right)$ **then**
        set $n=n+1$
        set $y^{k,n}=z$
        set *loop = false*
  set $y^{k+1}=\boldsymbol{A}_C\left(y^{k,N}\right)$
  set $k = k + 1$

Sufficient conditions for strong perturbation resilience of a Basic Algorithm were derived in [18, Theorem 1] and [19]. Along with the constraints $C \subseteq R^J$, we look at a target function $\phi : \Theta \subseteq R^J \rightarrow R$, with the convention that a point in R^J for which the value of ϕ is smaller is considered *superior* to a point in R^J for which the value of ϕ is larger. The essential idea of the superiorization methodology is to make use of the perturbations of (1) to transform a strongly perturbation resilient algorithm that seeks feasibility into an algorithm with an output that is equally good for constraints-compatibility but is also superior (not necessarily optimal) according to the target function ϕ.

The SM accomplishes its goal by producing from the Basic Algorithm another algorithm, called its *superiorized* version, that implements, at every iteration, a perturbation that reduces the target function value locally, i.e., $\phi\left(y^k + \beta_k v^k\right) \leq \phi\left(y^k\right)$. The Superiorized Version of the Basic Algorithm assumes that we have available a summable sequence $\{\eta_\ell\}_{\ell=0}^{\infty}$ of positive real numbers (for example, $\eta_\ell = a^\ell$, where $0 < a < 1$) and it generates, simultaneously with the sequence $\left\{y^k\right\}_{k=0}^{\infty}$ in Θ, sequences $\left\{v^k\right\}_{k=0}^{\infty}$ and $\{\beta_k\}_{k=0}^{\infty}$. The latter is generated as a subsequence of $\{\eta_\ell\}_{\ell=0}^{\infty}$, resulting in a nonnegative summable sequence $\{\beta_k\}_{k=0}^{\infty}$. The algorithm further depends on a specified initial point $y^0 \in \Theta$ and a positive integer N. It makes use of a logical variable called *loop*. Such a superiorized algorithm is presented here by its pseudo-code in Algorithm 1.

In general, the Superiorized Version of the Basic Algorithm outputs solutions that are essentially as constraints-compatible as those produced by the original (not superiorized) Basic Algorithm. However, due to the repeated steering of the process toward reducing the value of the target function ϕ, we can expect that the output of the Superiorized Version will be superior (from the point of view of ϕ) to the output of the original algorithm.

In recent years, the algorithmic structure of the superiorization method has undergone some evolution in ways that offer benefits in pCT. The details of this evolution can be found in the Appendix of [23], titled "The algorithmic evolution of superiorization".

A comprehensive overview of the state of the art and current research on superiorization appears in our continuously updated bibliography Internet page that currently contains 138 items [21]. Research works in this bibliography include a variety of reports ranging from new applications to new mathematical results on the foundations of superiorization. A special issue entitled: "Superiorization: Theory and Applications" of the journal Inverse Problems [24] contains several interesting papers on the theory and practice of SM. A special issue entitled: "Superiorization versus Constrained Optimization: Analysis and Applications" of the Journal of Applied and Numerical Optimization (JANO) appeared in 2020 [25].

A word About the history: The superiorization method was born when the terms and notions "superiorization" and "perturbation resilience", in the present context, first appeared in the 2009 paper of Davidi, Herman and Censor [20] which followed its 2007 forerunner by Butnariu et al. [26]. The ideas have some of their roots in the 2006 and 2008 papers of Butnariu et al. [27] and [28]. All these culminated in Ran Davidi's 2010 PhD dissertation [29] and the many papers since then cited in [21].

B. Derivative-free Superiorization (DFS) with Component-wise Perturbations

Superiorization reduces, but not necessarily minimizes, the value of a target function while seeking constraints-compatibility. When the perturbation steps are computationally efficient, the superior result is obtained with essentially the same computational cost as that of the original feasibility-seeking algorithm.

In the literature on superiorization, the perturbations that interlace target function reduction steps into the basic algorithm have, up to now, been done mostly by using negative gradients (or subgradients) directions and, thus, require some form of differentiability of the target function. In [30], we introduced *component-wise* perturbations that allow local non-ascent of the target function. These enable the SM to be applied with target functions that are *not* differentiable, similarly to such situations in optimization theory, where coordinate descent approaches are used.

The ramification of DFS for practical applications of the SM to IMPT treatment planning are meaningful. For example, normal tissue complication probability (NTCP), which is a predictor of radiobiological effects for organs at risk, should be used as an objective function in the mathematical problem modeling and the planning algorithm. Using NTCP or similar functions is hampered because these functions are, in general, empirical functions whose derivatives cannot be calculated, see, e.g., [31]. In a recent paper [32] the authors say that "...practical tools to handle the variable biological efficiency in Proton Therapy are urgently demanded..." highlighting this

need for the near future, but also in a longer perspective, of the proton therapy community.

By considering component-wise perturbations, we generalized previous superiorization schemes to enable the use of a more extensive selection of methods for step-wise reduction of the target function. As a first step in validating component-wise perturbations, we presented in [30] a new superiorization scheme for reducing total variation (TV) during image reconstruction from projections. More recently, this work has been continued in [33]. In that paper, DFS is put in context with the large field of derivative-free optimization (DFO) with many relevant references and a tool, called a "proximity-target curve", for deciding which of two iterative methods is "better" for solving a particular problem is developed. It is worthwhile to mention that other methodologies such as averaged stochastic gradient descent and automatic differentiation, that are widely used in optimization theory, in particular in the field of machine learning, also cope with lack of differentiability and employ "coordinate-wise" searches. There is certainly a potential to learn from the advances in these fields toward improving DFS.

C. The Fully-Discretized Problem Formulation of pCT Image Reconstruction

The water equivalent path length (WEPL) of a proton through an object, i.e., the length of the path the proton travels through water that leads to the same mean energy loss as in the object, can be expressed as a line integral of relative (to water) stopping power (RSP) along the path [34]. In practice, the object is described by a set of basis functions, and the integrals are expressed as discrete sums. This leads to a linear system $Ax = b$, where the ijth entry of the matrix A is the intersection length of the path of the ith proton with the jth voxel (basis function) and the ith component of the measurement vector b is the ith proton's measured WEPL. The mathematical formulation of the fully-discretized pCT reconstruction problem is: Given A and b, estimate x.

The system matrix A is generated by calculating the path length through each basis function (normally a voxel). Different from the straight-line assumption in x-ray CT, in pCT, discrete steps along most likely path (MLP) approximations developed in [35], created by multiple small-angle Coulomb-scattering of protons in the object, are used. Thus, proton paths through the reconstructed object are approximated at a finite set of points along each MLP. Employing a linear path approximation through individual basis functions simplifies the calculation. It is justified by the minor deviation of a proton path from a straight line on the scale of the voxel dimension (1-2 mm). However, the need to identify intersection lengths of protons through individual voxels creates high computational demand with the need to identify intersection lengths of millions of protons through millions of voxels. We addressed this problem by using GPGPUs (general-purpose graphics processing units) that perform calculations that would otherwise typically be conducted by the CPU (central processing unit). Such GPGPUs were used for the implementations of pCT reconstruction codes (see Subsection III-A below).

D. A New Algorithm for TV-Superiorized (TVS) pCT Image Reconstruction

The efficacy of the SM for image reconstruction in pCT has been shown in previous work [36]. In that work, we superiorized the total variation (TV) as the target function to improve pCT image quality. The usefulness of TVS was demonstrated for pCT image reconstruction with different superiorized versions of the block-iterative diagonally relaxed orthogonal projections (DROP) algorithm [37]. Two TVS schemes added-on to DROP were investigated; the first carried out the superiorization steps once per cycle and the second once per block.

A new version of the TVS algorithm, referred to as NTVS (New TVS), was investigated in [38]. Compared to the original TVS algorithm published by Penfold et al. in [36], the NTVS includes several structural changes and new aspects previously not investigated. It combines properties that were scattered among previous works on TVS in x-ray CT but were never combined in a single algorithm, neither for x-ray CT nor for pCT. These properties are: (1) exclusion of the TV reduction verification step; (2) usage of powers of a perturbation kernel α to control the step-sizes β_k in the TV perturbation steps; (3) incorporation of the user-chosen integer N that specifies the number of TV perturbation steps between consecutive feasibility-seeking iterations; and (4) incorporation of a new formula for calculating the power of α that is used to calculate the step-size of the perturbation steps. The notation and other algorithmic details of the NTVS algorithm can be found in [38].

E. Adding Robustness to pCT Image Reconstruction

Imaging systems commonly contain some uncertainty in modeling and measurement. For pCT, there is uncertainty in the estimated MLP and the measurement of the WEPL of individual protons. In standard algorithms, this uncertainty, often measured by the residuals $r = \| b - Ax \|$, is considered part of the measurements b rather than the modeled system Ax. In robust systems, errors are modeled as part of both the system matrix A (in pCT, intersection length of individual proton MLPs with individual voxels) and the measurement vector b (in pCT, the WEPL). Methods such as total least squares, ridge regression, and Tikhonov regularization are classic techniques for robust systems, and all can be solved as a diagonal perturbation to the normal equations of least squares, see for example [39]. The main difference relates to the regularization parameter, which is typically a small number related to the uncertainty parameter, and bounds on A and b. A more recent technique, Bounded Data Uncertainty (BDU) models the uncertainty as perturbations E, to the matrix A, such that the actual system is $(A+E)x$. The perturbations are bounded such that $\|E\| \leq \eta$. For the worst case perturbations [40] and [41] and best case perturbations [42] and [43] the resulting problem is solved by $x = (A^t \Phi A + \Psi)^{-1} A^T \Phi b$, which again can be solved by a diagonal perturbation to the normal equation of least squares. In BDU, the perturbation to the diagonal is dependent on the solution and must be solved for iteratively using a "secular equation," which is

a one dimensional, nonlinear equation involving uncertainty parameter η, and bounds on A and b. These diagonal perturbations can be thought of as perturbing the singular values of the underlying system of A and b. Analogously, in [44], we introduced the *fully-simultaneous adaptive iterative solver* (FSAIS) for the fully-discretized problem formulation of pCT image reconstruction and provided a convergence analysis. To obtain a sparse robust solution, we formed the augmented linear system

$$\begin{bmatrix} -\Psi & A^T \\ A & \Phi^{-1} \end{bmatrix} \begin{bmatrix} x \\ r \end{bmatrix} = \begin{bmatrix} 0 \\ b \end{bmatrix}, \tag{2}$$

where A, x, and b are defined as in II-C, and the choice of the matrix parameters Ψ and Φ is discussed below. Solving the top equation for x and the second equation for r, one obtains the following system of equations:

$$r = \Phi\left(b - Ax\right), \tag{3}$$

$$x = \Psi^{-1}A^T r, \tag{4}$$

which reduces to

$$x = \Psi^{-1}A^T\Phi\left(b - Ax\right). \tag{5}$$

This equation opens a formal way of selecting an iterative algorithm that leads to robust RSP values. Given a current iteration vector x^k, the FSAIS generates the next iteration vector x^{k+1} by

$$x^{k+1} = x^k + \Psi^{-1}A^T\Phi(b - Ax^k). \tag{6}$$

Since many robust methods result in diagonal perturbations with values that typically lie in a similar area, in FSAIS the two diagonal parameter matrices Ψ and Φ are free parameters that can be adjusted for robustness and speed of convergence. The parameter Φ handles normalization and weighting between the rows of A and b. The parameter Ψ includes the relaxation paramter and adjusts weighting between the uncertainty η, the elements of x, and the matrix A. Our choices for these parameters are $\Phi_i := \frac{1}{\|A_i\|^2}$, where A_i is the ith row of the matrix A, and $\Psi_j^{-1}(k) := (1 - x_j^k)\lambda(k)$, where $\lambda(k)$ is the relaxation parameter at the kth iteration and x_j^k is the jth component of the kth iteration vector. In a pCT reconstruction study with the Catphan® CTP404 sensitometry module (The Phantom Laboratory, Inc., Salem, NY), which contains cylindrical inserts with a wide range of RSP, FSAIS was shown to obtain results similar to the DROP algorithm of [37] for RSP values near 1 but obtained significantly better results than DROP for denser materials (RSP>1) such as acrylic (1.160), Delrin® (1.359), and Teflon® (1.790). FSAIS was also able to handle missing data, i.e., proton histories in an angle interval being removed. This was done to simulate situations, for example, where protons cannot penetrate individual body sections because the proton energy would not be sufficient. Using the filtered back projection (FBP) reconstruction along straight proton paths as the initial iterate, FSAIS stayed within 2% of the RSP for up to 60 degrees of lost data and was within 1% for almost all materials for 30 degrees of lost data.

F. Development of a Motion-Adapted Iterative Reconstruction Algorithmic Framework for pCT

In the past and up to now, it was assumed that the object that undergoes pCT imaging is static throughout the pCT data acquisition. However, this is not the case when imaging, for example, the lungs because, during the image acquisition, the acquired data belong to different motion states at different specific time instances. It is important to note here that we register individual protons with a time tag during the data acquisition process. During the data acquisition, one can also measure a surrogate breathing signal that gives information about the tidal volume of the lungs. Common concepts in four-dimensional-CT (4D-CT) imaging with the registration of the breathing motion are those of a "reference state" and the "reference image" which represent the patient lungs in a specific state of filling and, typically, at rest, respectively, for example, at the end of normal expiration when the breathing airflow ceases for a moment. In the work-in-progress described next, we developed and investigated an algorithmic framework that enables the reconstruction of the reference image of a breathing patient assuming that the tissue motion can be described by accurate deformation vector fields, see, e.g., [45]. For ordinary (motion-free) pCT data acquisition, one uses a detector-fixed coordinate system for tracking discrete proton coordinates for MLP calculation and an object-fixed coordinate system for reconstructing the RSP; both coordinate systems are represented by a regularly spaced, three-dimensional voxel grid [46]. When motion is present, the object-fixed voxel grid is only regular for the reference state. However, it is deformed for all other motion states according to the deformation described by the motion model. The general reconstruction equation $Ax = b$ is retained because motion only influences the A-matrix elements according to the MLP intersection length of the deformed grid cells. Assuming that the RSP values of the deformed grid cells are retained (an approximation), the reconstructed image corresponds to the reference image when the solution vector is assigned to the rectangular voxel grid, and any other motion state when it is assigned to the deformed grid of that motion state.

We define a "motion model," in the context of pCT image reconstruction, to be a system (like a blackbox) capable of describing the three-dimensional (3D) spatial displacement of human moving tissues at any time instance relative to their reference position. To make this statement more concrete, we consider a 3D regular voxel grid fixed in the object-fixed coordinate system whose voxel centers are, for each voxel j, at the 3D position vector $\overrightarrow{X}_0^{(j)}$. For every voxel index, $j = 1, 2, \ldots, J$, the pair $(y_0^{(j)}, \overrightarrow{X}_0^{(j)})$ represents the relative stopping power (RSP) of the voxel j, denoted by $y_0^{(j)}$, and the location $\overrightarrow{X}_0^{(j)}$ of the voxel center in the reference image, see Figure II.1.

According to the modeled displacement of the object tissues due to motion, at time t, the pair $(y_0^{(j)}, \overrightarrow{X}_0^{(j)})$ becomes $(y_0^{(j)}, \overrightarrow{X}_t^{(j)})$, meaning that the RSP value $y_0^{(j)}$ remains unchanged, but its reference point has moved to a new spatial location $\overrightarrow{X}_t^{(j)}$, not necessarily conforming with the original fixed grid, as determined by the nature of a transformation T

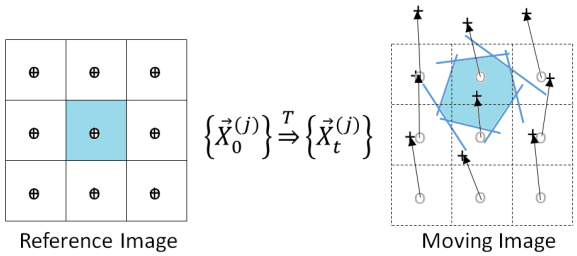

Fig. II.1. Two-dimensional schematic of the reference image (left) with a regular system of points marking the centers of an object-centered fixed voxel grid $j = 1, 2, \ldots, J$. In the moving image (right), the position of the original voxel center points have shifted as a whole (translation) and relative to each other (deformation) to new locations due to tissue motion, which is described by a deformation vector field T. The blue-shaded regions are Voronoi cells (see text for details).

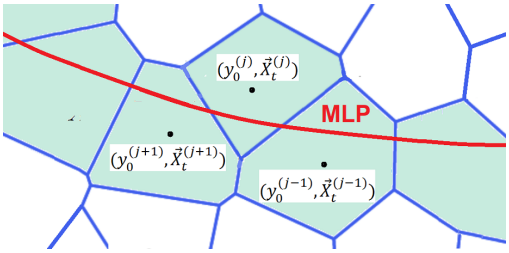

Fig. II.2. Two-dimensional schematic of the pCT reconstruction problem of a moving organ at a specific time instance t when the organ is represented by the Voronoi cell basis functions shown. The most likely path (MLP) of an individual proton intersects the shaded cells. The summation of the intersection lengths of the ith MLP with the jth voxel, a_{ij} multiplied by the unknown RSP values y_0^j of each cell is set equal to the ith component of the b vector of measured WELP values, and thus form a linear system of equations $Ay_0 = b$ that is solved iteratively for the reference image vector y_0 by a feasibility-seeking algorithm.

described by a deformation vector field that is, in general, not repeatable nor periodic and is described by the motion model.

Our motion-adapted pCT reconstruction makes use of the concept of Voronoi diagrams and cells, see, e.g., [47, Subsection 5.5], [48]. We use the following definition.

Definition 1. *Let $P := p_1, p_2, \ldots, p_J$ be a set of J voxel center points (called sites) in the 3D reference image space and let dist(p_j, p_k) denote the Euclidean distance between voxel center point p_j and any other voxel center point $p_k, k \neq j$. The "Voronoi diagram" of P, is defined as the partition of the 3D space into J connected 3D cells (called "Voronoi cells" or "Voronoi polygons") such that any point q in the image space belongs to the Voronoi cell corresponding to a site p_j if and only if dist$(q, p_j) <$ dist(q, p_k) for each $p_k \in P$ with $k \neq j$.*

It is understandable from Figure II.1, when expanded into the third spatial dimension, that boundaries of Voronoi cells are formed by plane sections that are created by the intersection of bisecting half-spaces between pairs of sites, line segments formed by the intersection of these planes, and vertices formed by the intersection of two or more of these line segments. The "bisecting plane" of two points p and q is the plane that is perpendicular to the line segment $\overline{pq}$ and intersects it at the midpoint. This bisecting plane divides the 3D space into two half-spaces. Then the Voronoi cell of point p_k, denoted by $\mathcal{V}(p_k)$, is

$$\mathcal{V}(p_k) = \bigcap_{j \neq k, j=1}^{J} h(p_k, p_j), \tag{7}$$

where $h(p_k, p_j)$ is the bisecting plane of the points (p_k, p_j).

In our approach to motion-adapted pCT reconstruction, which is illustrated in Figure II.2, the Voronoi cells become the new basis functions, and the originally formulated fully-discretized problem of pCT reconstruction remains unchanged. The specific Voronoi cell basis functions depend on the motion state of the tissues, which is described by a motion model. The motion model allows calculation of the displacement vector for individual voxel points at any given instance of time. The new positions of the voxel points are used to compute the plane segments of the Voronoi cells. Together with an MLP algorithm, one can then calculate the intersection length of the ith proton through the jth Voronoi cell basis function, and the ith component of the WEPL measurement vector b gives the ith proton's measured WEPL. This results in a linear system of equations that is solved iteratively by a feasibility-seeking algorithm. The unknown RSP values of each cell are assumed not to change from their values in the reference image. Thus, the reconstructed voxel image where each voxel is assigned the reconstructed RSP value $y_0^{(j)}, j = 1, 2, \ldots, J$, corresponds to the reference image. One can also calculate the image at any point in time by calculating a weighted average of the RSPs with weights that are proportional to the area a voxel shares with overlapping Voronoi cells.

The motion model parameters could be known at the time of pCT imaging from a separate motion imaging study, or they could be included in the image reconstruction problem and estimated after the imaging. By way of example only, we mention here the lung motion model originally developed by Low and colleagues [49], [50]. This model has recently been applied in conjunction with an iterative projection algorithm for a motion-compensated simultaneous algebraic reconstruction technique (MC-SART) of cone beam CT (CBCT) [51], [52]. There is, however, a fundamental conceptual difference between our approach and the MC-SART algorithm. To "handle" the motion, the authors modified the reconstruction algorithm (SART in their work) while we, to handle the motion, modify the problem (the linear system of equations in our work). Our approach is, therefore, general in the sense that once the problem is appropriately modified to handle the motion, one can apply any iterative algorithm to the "modified problem." Our framework can take the output of any motion model as input to the algorithm for computation of the basis functions at each instance in time when proton histories are acquired. The motion model and the algorithm are, thus, two separate entities that have to be used in tandem when applied to simulated or real data.

Besides the motion model of Low et al., other motion models exist, see, e.g., [53]–[55].

Fig. II.3. Profile of a voxel (a) and a blob (b).

G. Blob Basis Functions for pCT Image Reconstruction

"Blob" basis functions, called "radial basis functions" in approximation theory, see, e.g., [56], are spherically symmetric basis functions for CT reconstruction that were suggested in the field of image reconstruction from projections by Lewitt in the early 1990s [57], [58]. These blobs are generalizations of a well-known class of functions used in digital signal processing called Kaiser-Bessel window functions and they yield excellent results in multiple imaging modalities, see, e.g., the enlightening tutorial by Herman [59]. Matej and Lewitt [60], [61] provided a careful investigation of how the blob basis functions should be chosen when they are used in the context of image reconstruction from projections. Since then blobs have been used extensively for image reconstruction in X-ray computerized tomography, positron emission tomography, single photon emission computerized tomography, optoacoustic tomography and electron microscopy (consult [59] for references and details). Adhering to the term "blobs", as commonly used in this field, we have started to develop a methodology for using blobs instead of standard square voxels in pCT. The use of blobs will potentially improve pCT image quality and computational efficiency.

Current pCT makes use of conventional voxels for reconstructing and representing reconstructed images. However, proton paths through the reconstruction object are curved and must be approximated at a finite set of points along each path. The computational burden to identify intersection lengths of protons through individual voxels is quite large, especially when the object elements are not spatially invariant. Using blobs as a replacement of voxels in pCT can significantly reduce this computational burden because of the spherical symmetry of the blobs. We presented initial encouraging results in collaboration with UCLA graduate student Howard Heaton as a poster at the 2016 Joint Mathematics Meetings (JMM) [62].

Voxels have a uniform value inside a set domain, and blobs are spherically symmetric and taper smoothly to zero at their border, see Figure II.3. The formal definition for blob basis functions for CT imaging, first proposed by Lewitt [58], is as follows:

$$b_j(r) := \begin{cases} \frac{\left[1-(r/a)^2\right]^{m/2}}{I_m(\alpha)} I_m\big(\alpha\sqrt{1-(r/a)^2}\big), & \text{if } r \in [0,a], \\ 0, & \text{otherwise,} \end{cases} \tag{8}$$

where b_j is the basis function of the jth blob, r is the radial distance from the center of the jth blob, I_m denotes the modified Bessel function of the first kind of order m, a denotes the radius of the blobs, and α is a nonnegative real number that controls the shape and taper of the blob. It is common practice to choose $m = 2$, which gives a smooth and differentiable blob function. Following Benkarroum et al. [63], we have chosen the blob parameters to be $a = 2.453144$ mm and $\alpha = 13.738507$. Those parameter values were chosen for optimal representation of piecewise-constant images.

To generate the system matrix A, the path length through each basis function must be computed. Employing a linear path approximation through individual basis functions (voxels or blobs) allows the use of the Radon transform $\mathcal{R}$ to approximate each entry A_{ij}, i.e.,

$$A_{ij} = \int_{path} b_j(\vec{s}\ )\ d\vec{s}\ \approx\ [\mathcal{R}b_j](\ell_i, \theta_i), \tag{9}$$

where

$$[\mathcal{R}b_j](\ell_i,\theta_i) = \int_{line} b_j\left(\sqrt{\ell_i^2+z^2},\ \theta_i + \tan^{-1}\left(z/\ell_i\right)\right)\ dz \tag{10}$$

is the Radon transform of the straight-line approximation of the path through the blob. Note that with blobs, the Radon transform depends solely on perpendicular distance from the blob center, ℓ_i.

To construct the system matrix, we use the following problem formulation.

Problem 1. ***Generation of the A-matrix for blob basis functions****: Let $\{\vec{\varphi}^{\,\ell}\}_{\ell=1}^{L}$ denote an ordered set of points along a proton path in $\mathbb{R}^3$. Suppose that this path passes through an object represented with a set $\{b_j\}$ of blob basis functions. Using successive points $\vec{\varphi}^{\,\ell}$ along the path, uniquely estimate each nonzero blob intersection length of the path to generate the corresponding system matrix.*

A key step in the algorithm presented in [62] is to identify blobs within a given proximity of a point $\vec{\varphi}^{\,\ell}$ on the path. This is accomplished by identifying a corresponding point $\vec{\Phi}^{\,\ell}$ located nearby on the grid of blob centers with grid unit β. The algorithm identifies each nonzero blob intersection length by identifying a blob in proximity to $\vec{\varphi}^{\,\ell}$. Then the algorithm begins to cycle through nearby blobs within a chosen range κ. Finally, it restricts intersection lengths to being assigned during the last step the proton takes before passing the blob center in depth. Further details can be found in [62].

H. Algorithms for IMPT: Dose-volume Constrained Split Feasibility

IMPT is a rapidly developing field wherein active pencil beam scanning became the norm in proton and ion beam treatment centers. IMPT requires scanning of a particle treatment field with a grid of pencil beam spots that are rapidly and often repeatedly "visited" during the treatment to deliver a spot dose with varying intensity. Such a scan demands fast IMPT algorithms that solve the inverse problem with multiple dose constraints within target volumes and organs at risk. During our research, we tackled the additional complication that dose constraints are often modified, by the treatment planner, allowing violation of the constraints by a specific percentage of the dose for a specific percentage of the volume. The method we developed to handle this is also useful for x-ray IMRT, see [64].

The linear feasibility problem (LFP) formulation, which is a special case of the well-known convex feasibility problem (CFP), see, e.g., [1], forms a basic model for the inverse problem in the fully-discretized approach to both IMPT and IMRT treatment planning. In 2015, we showed that IMPT inverse planning is possible by using a fully-discretized model and a feasibility-seeking algorithmic approach [65]. In particular, we demonstrated on a simple 2D example that solutions meeting the planning objectives could be found by these feasibility-seeking iterative projection algorithms.

In the planning of IMPT or IMRT, one uses dose-volume constraints (DVCs) to evaluate treatment plans. Mathematically, DVCs are percentage-violation constraints (PVCs). PVCs single out individual subsets of the existing volume constraints and allow a specified percentage of dose constraints to be violated in each subset. Without incorporating the PVCs into the mathematical inverse planning model and algorithm themselves, it is not possible to guarantee that an appropriate solution will be found [64].

A tractable model and an algorithmic approach to solve the IMPT/IMRT inverse planning problem as a feasibility problem that includes DVCs has been developed. A rigorously defined notion of PVCs cause integers to enter the problem, which makes it difficult to solve. To circumvent this difficulty, we reformulated the PVC with the aid of a "sparsity-norm" that counts the number of nonzero entries in a vector. There is a rich literature on how to handle this norm, called also the ℓ_0-norm, which is still stimulating recent and ongoing related work. It is not in the scope of this paper to review this field but see, e.g., [66] and its references, where the problem is formulated and handled as a full fledged constrained optimization problem. Using the ℓ_0-norm enables to enforce the DVCs and leads to redefining the "linear feasibility problem with PVCs" as another feasibility problem that includes non-convex constraints for the sparsity-norm.

Problem 2. *[64]* ***Linear Interval Feasibility with DVC for the inverse problem in the fully-discretized approach to IMRT treatment planning****. Find $x^* \in R^n$ for which*

$$0 \leq A_1 x \leq (1+\beta)b^1, \tag{11}$$

$$b^3 \geq A_2 x \geq b^2, \tag{12}$$

$$0 \leq A_3 x \leq b^4, \tag{13}$$

$$x \geq 0, \tag{14}$$

$$\|(A_1 x - b^1)_+\|_0 \leq \alpha m_1, \tag{15}$$

where $A_1 \in R_+^{m_1 \times n}$, $A_2 \in R_+^{m_2 \times n}$, $A_3 \in R_+^{m_3 \times n}$ are given matrices, $b^1 \in R_+^{m_1}$, $b^2, b^3 \in R_+^{m_2}$, $b^3 \in R_+^{m_3}$ are given vectors, and $\beta > 0$ and $\alpha \in [0,1]$ are given real numbers.

In this problem, applicable to both IMPT and IMRT, the sparsity constraint (15) takes place in the space R^{m_1}, where the vectors of doses in the organs at risk reside. Therefore, we cannot use plain feasibility-seeking methods but need feasibility-seeking methods for "split feasibility problems." Thus, we recognized that Problem 2 is a split feasibility problem. Split feasibility problems were introduced first in [67] and further studied in [68], [69] and many other publications. The reader may consult the brief review of "split problems" formulations and solution methods in [70] for more details and references. For the solution of Problem 2, which includes a non-convex sparsity-norm induced constraint, we developed a new iterative projection algorithm, which is a combination of the CQ-algorithm [71] and the automatic relaxation method (ARM) [72]. Full details of this approach appear in [64], which applied it to a single OAR. Following this line of development, we expanded the model to include DVCs for several OARs in a more recent paper [70]. Handling DVCs in radiation therapy treatment planning is a viable research area and a variety of techniques have been applied to solve it, see, e.g., [73] and references therein.

III. Development of software tools and phantoms to test advanced pCT and IMPT algorithms

The demand for high-performance computing capabilities for pCT image reconstruction and IMPT algorithm development, is apparent. In this section, we summarize developments facilitating fast algorithms for pCT and IMPT.

A. GPGPU Data Partitioning

An essential aspect of our work as members of the pCT collaboration has been to provide tools for fast and efficient image reconstruction using GPGPU computations. The pCT detector hardware was developed in two phases from a fairly small and slow detector system in Phase I to a much faster Phase II system completed in 2015 [74]. As the reconstructed image gets larger, the number of proton histories that enter the reconstruction is up to one hundred times the number of voxels in the image, see [75]. Currently, objects requiring a six minutes scan time (up to 360 million proton histories) with the "Phase II proton CT scanner" can be reconstructed on the order of a few minutes [76]–[78]. As we image larger objects with protons, not only does the reconstruction time grow significantly, but, more importantly, the memory requirements grow too. Therefore, we need to split the data into coherent data blocks for efficient reconstruction. Since the Phase II pCT scanner acquires the data during a 360-degree rotation of the object relative to the pCT scanner with a wobbled or scanned beam spot [77], [79], we can efficiently split the data into slices orthogonal to the rotational axis, see [78].

For a nominal proton entrance energy of 200 MeV and a few tens of MeV exit energy, proton path histories within three standard deviations of the nominal path in lateral direction do not pass through more than three 1 mm slices. So, when reconstructing a slice, no more than three slices above or below the slice need to be available in memory of a particular GPGPU to reconstruct the image efficiently, see [80]. When reconstructing slice-by-slice, we can allocate up to one GPGPU per slice. For proton histories passing through multiple slices, each GPU associated with a slice holds the most recent copy of the RSP values of adjacent slices. Updates from adjacent slices are transferred when the thread calculating the update finishes an iterative cycle of the algorithm.

The results presented in [78], [80] show that this method does not cause a significant image quality reduction while

permitting reconstruction of the anthropomorphic head phantom described below in under 10 minutes on NVIDIA P100 GPGPUs. Further speedup to reconstruction in under 1 minutes is within reach.

B. Monte Carlo Simulation Tools

Monte Carlo (MC) simulations are an essential tool in the development and testing of algorithms for pCT image reconstruction and serve as a forward calculation tool for the radiation dose deposited in object voxels of IMPT plans. While testing algorithms on real-world experimental data is equally important, MC-based data are more readily available and provide a great deal of flexibility when testing and developing new algorithms or algorithmic variants.

We have made extensive use of the general-purpose MC simulation tool Geant4 [81] to develop a faithful model of the Phase II pCT detector system developed by the pCT collaboration (see Section III-A). For this project, we reproduced the exact geometry and composition of materials of the scanner as well as the research proton beamline at the Loma Linda University Medical Center. Details of the initial Geant4 platform development and the methods we used to validate its output, in connection with reconstruction algorithms that we developed, can be found in Dr. Giacometti's thesis publications, see [82]. We then used pCT simulations produced by that platform in addition to experimental data to test the performance of the new TVS algorithms described in Section II-A.

Later, we implemented the Phase II scanner in the TOPAS (**TO**ol for **PA**rticle **S**imulation) platform, which is also based on the Geant4 toolkit but has a more user-friendly interface [83]. We also tested the Phase II pCT scanner at the Northwestern Medicine Chicago Proton Center (NMCPC), where it is operated on a clinical proton beamline. The TOPAS model of the NMCPC beamline was validated with beam profile measurements acquired at NMCPC and by acquiring and simulating pCT images using a wobbled 200 MeV proton beam. With the TOPAS tool, we then investigated the sources of systematic uncertainty introduced during the steps of iterative RSP reconstruction with the DROP-TVS algorithm [36] for CT QA phantom modules (Catphan®, The Phantom Laboratory Incorporated, Salem, NY, USA) and a digital representation of a pediatric patient with known ground truth RSP values in the simulation, see [84]. The important point here is that with Monte Carlo simulations of the pCT system performance, we can intentionally include or exclude different sources of random and systematic uncertainties that arise from random fluctuations in the proton energy loss and scattering, which are unavoidable, and sources of imperfections in the beam source or the detector construction. For example, we had to understand the origin of ring artifacts seen in the reconstruction of homogeneous phantoms. Through systematic Monte Carlo studies, we learned that these artifacts were related to using a WEPL calibration phantom with discrete thickness steps. A simulation of the pCT detector replacing the step phantom with a wedge phantom demonstrated that the ring artifacts could be significantly reduced [84].

At the end of 2016, we shipped the Phase II pCT scanner to the Heidelberg Ion Therapy (HIT) Center in Germany for first experiments with helium ion imaging. Again, TOPAS was used to simulate helium CT data for predicting and evaluating the characteristics of HeCT images reconstructed with the DROP-TVS algorithm now in comparison with proton CT images, see [85]. Given the ease and accuracy of results, it is thus a "natural" choice to use TOPAS for forward dose calculations when testing new IMPT algorithms.

C. Digital Phantoms

Another critical need is to identify or develop anthropomorphic digital phantoms necessary for realistic pCT and IMPT algorithm testing. The general strategy we have followed for most of the algorithms we have tested has been to demonstrate the algorithmic idea with several phantoms ranging from simple phantoms often in two dimensions to increasingly larger and more realistic phantoms. We believe that this approach prevents the "masking" of the principal numerical performance of new algorithms by difficulties stemming from the complexity of realistic object data, which may require different adjustments after the performance of the algorithms has been demonstrated on simpler datasets. In the following paragraph, we describe the digital head phantom that we specifically designed to support our pCT algorithmic developments.

Head Phantom: We created the HIGH_RES_HEAD digital head phantom with very high resolution, [86] for the development and evaluation of pCT image reconstruction algorithms and IMPT algorithms, but it can be used for other medical physics purposes as well. The phantom is now available as a computational DICOM head phantom to the Geant4 user community in the open source Geant4 MC simulation tool package [87]. The phantom represents a head of a 5-year-old child. It is a very close approximation of the commercial head phantom (model HN715, CIRS, Norfolk, VA, USA). The HIGH_RES_HEAD digital phantom includes most anatomical details of a human head and is characterized by a high spatial resolution ($0.18 \times 0.18 \times 1.25\ mm^3$ voxel size). We used it together with the Geant4 simulation platform of the pCT system to validate its performance by comparing digital phantom reconstructions with reconstructions from experimental data [88]. The phantom was also used for testing the parameter space of a novel superiorization algorithm for pCT reconstruction [38], described in Subsection II-D above. Figure III.1 shows a representative proton CT reconstruction from that work.

IV. The Loma Linda University algorithm workshops

We have organized, since 2015, five "Loma Linda University (LLU) Workshops on Algorithms and Computational Techniques in Proton Imaging and Intensity-Modulated Proton Therapy." For details about the previous and planned Annual Loma Linda workshops, see http://ionimaging.org/. The first three workshops were face-to-face meetings at LLU, Loma Linda, CA, USA, during the weeks following the annual meetings of the American Association of Physicists in Medicine

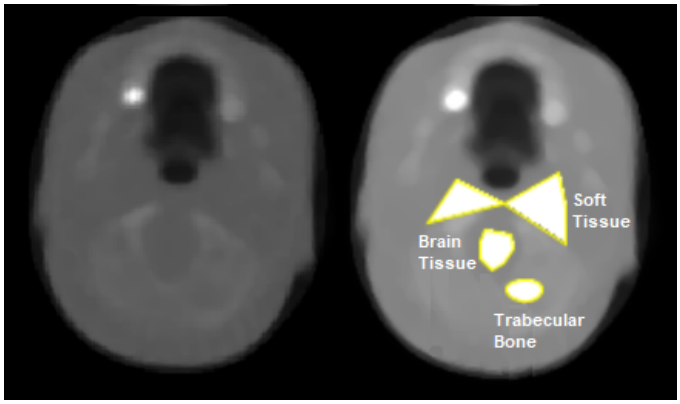

Fig. III.1. Representative pCT reconstruction of the slice of the pediatric head phantom containing regions of interest (left); the regions of interest are filled in white and labeled by their composition (right). (reproduced from [38]).

(AAPM). Participation was by invitation only, and we welcomed applied mathematicians, computer scientists, medical physicists, radiobiologists, and radiation oncologists. We have organized the workshops in an informal setting: there were no workshop fees, no parallel sessions, and no strictly timed talks. The emphasis was on scientific exchange, learning, and discussions. In all workshop meetings, the participants learned from each other, and new research projects and collaborations have emerged that are still on-going. For the 4th and 5th workshops, we also allowed participation by video-conferencing via Zoom, and the 6th workshop in July 20-22, 2020, was a Zoom-only workshop due to the COVID-19 pandemic. The 7th workshop was held in August 2-4, 2021 at Loma Linda via Zoom, see: http://ionimaging.org/llu2021-overview/.

V. Discussion and Conclusion

When it comes to advanced techniques such as pCT and IMPT, there is a strong need for input from experts in computer science and mathematics to support the medical physicist's insight and understanding. With this in mind, we collaborate on developing advanced reconstruction algorithms for pCT imaging based on mathematical expertise in iterative projection methods. With computer science expertise, we have achieved progress and fast implementation of novel mathematical algorithms on advanced computing hardware. There is still much more to accomplish with increasing demands for high-speed and high-performance medical imaging and verification techniques leading to online-adaptive particle therapy, the inclusion of biological weighting in treatment planning optimization or superiorization, and a combination of different image guidance technologies such as MRI and pCT. Such interdisciplinary collaboration should stimulate others to follow a similar path and widen the network of collaborations in the disciplines of medical physics, mathematical algorithms, and computer science.

Appendix

Acknowledgments. We thank the many collaborators on the projects mentioned here, in particular, Blake Schultze, Paniz Karbasi, Caesar Ordonez, Christina Sarosiek, Howard Heaton, Jose Ramos-Mendez, Pierluigi Piersimoni, Robert Jones, Robert Johnson, Stuart Rowland, and Tai Dou as well as Mark Pankuch and his medical physics and accelerator support team at the Northwestern Medicine Chicago Proton Center for help with collecting proton CT data with the Phase II pCT scanner. The interdisciplinary efforts described here were supported by the United States-Israel Binational Science Foundation (BSF) ([89], [90]). The work of Y.C. was supported by the ISF-NSFC joint research program grant No. 2874/19. All authors contributed equally to the writing of this paper. All authors read and approved the final manuscript. We appreciate the anonymous reviewer's report which helped us improve the paper.

References

[1] H. H. Bauschke and J. M. Borwein, "On projection algorithms for solving convex feasibility problems," *SIAM Review*, vol. 38, pp. 367–426, 1996.

[2] C. L. Byrne, *Applied Iterative Methods*. A. K. Peters Ltd., Wellesley, MA, USA, 2008.

[3] J. W. Chinneck, *Feasibility and Infeasibility in Optimization: Algorithms and Computational Methods*. International Series in Operations Research & Management Science, Springer Science+Business Media, LLC, 2008.

[4] Y. Censor and S. A. Zenios, *Parallel Optimization: Theory, Algorithms, and Applications*. Oxford University Press, New York, NY, USA, 1997.

[5] D. Butnariu, Y. Censor, P. Gurfil, and E. Hadar, "On the behavior of subgradient projections methods for convex feasibility problems in Euclidean spaces," *SIAM Journal on Optimization*, vol. 19, pp. 786–807, 2008.

[6] C. Byrne and Y. Censor, "Proximity function minimization using multiple Bregman projections, with applications to split feasibility and Kullback–Leibler distance minimization," *Annals of Operations Research*, vol. 105, pp. 77–98, 2001.

[7] Y. Censor, A. R. De Pierro, and M. Zaknoon, "Steered sequential projections for the inconsistent convex feasibility problem," *Nonlinear Analysis: Theory, Methods & Applications*, vol. 59, pp. 385–405, 2004.

[8] Y. Censor, A. Motova, and A. Segal, "Perturbed projections and subgradient projections for the multiple–sets split feasibility problem," *Journal of Mathematical Analysis and Applications*, vol. 327, pp. 1244–1256, 2007.

[9] H. H. Bauschke and V. R. Koch, "Projection methods: Swiss army knives for solving feasibility and best approximation problems with halfspaces," *Contemporary Mathematics*, vol. 636, pp. 1–40, 2015.

[10] A. Brahme, J.-E. Roos, and I. Lax, "Solution of an integral equation encountered in rotation therapy," *Physics in Medicine and Biology*, vol. 27, pp. 1221–1229, 1982.

[11] M. D. Altschuler and Y. Censor, "Feasibility solutions in radiation therapy treatment planning," *In: Proceedings of the Eighth International Conference on the Use of Computers in Radiation Therapy*, pp. 220–224, 1984.

[12] Y. Censor, M. D. Altschuler, and W. D. Powlis, "A computational solution of the inverse problem in radiation-therapy treatment planning," *Applied Mathematics and Computation*, vol. 25, pp. 57–87, 1988.

[13] ——, "On the use of Cimmino's simultaneous projections method for computing a solution of the inverse problem in radiation therapy treatment planning," *Inverse Problems*, vol. 4, pp. 607–623, 1988.

[14] Y. Censor, W. D. Powlis, and M. D. Altschuler, "On the fully discretized model for the inverse problem of radiation therapy treatment planning," *in: Proceedings of the Thirteenth Annual Northeast Bioengineering Conference, (K. R. Foster, Editor), Institute of Electrical and Electronics Engineers (IEEE), New York, NY, USA*, vol. 1, pp. 211–214, 1987.

[15] T. Bortfeld, J. Bürkelbach, R. Boesecke, and W. Schlegel, "Methods of image reconstruction from projections applied to conformation radiotherapy," *Physics in Medicine & Biology*, vol. 35, pp. 1423–1434, 1990.

[16] Y. Censor, "Mathematical aspects of radiation therapy treatment planning: Continuous inversion versus full discretization and optimization versus feasibility," *In: Computational Radiology and Imaging: Therapy and Diagnosis, C. Börgers and F. Natterer (Editors), The IMA Volumes in Mathematics and its Applications, Vol. 110, Springer-Verlag, New York, NY, USA*, pp. 101–112, 1999.

[17] P. S. Cho and R. J. Marks II, "Hardware-sensitive optimization for intensity modulated radiotherapy," *Physics in Medicine and Biology*, vol. 45, pp. 429–440, 2000.

[18] G. T. Herman, E. Garduño, R. Davidi, and Y. Censor, "Superiorization: An optimization heuristic for medical physics," *Medical Physics*, vol. 39, pp. 5532–5546, 2012.

[19] Y. Censor, R. Davidi, G. T. Herman, R. W. Schulte, and L. Tetruashvili, "Projected subgradient minimization versus superiorization," *Journal of Optimization Theory and Applications*, vol. 160, pp. 730–747, 2014.

[20] R. Davidi, G. T. Herman, and Y. Censor, "Perturbation-resilient block-iterative projection methods with application to image reconstruction from projections," *International Transactions in Operational Research*, vol. 16, pp. 505–524, 2009.

[21] Y. Censor, "Superiorization and perturbation resilience of algorithms: A bibliography compiled and continuously updated," *Available at: http://math.haifa.ac.il/yair/bib-superiorization-censor.html#top*.

[22] Y. Censor, R. Davidi, and G. T. Herman, "Perturbation resilience and superiorization of iterative algorithms," *Inverse problems*, vol. 26, no. 65008, 2010.

[23] Y. Censor, "Can linear superiorization be useful for linear optimization problems?" *Inverse Problems*, vol. 33, p. 044006, 2017.

[24] Y. Censor, G. T. Herman, and M. Jiang, Eds., *Superiorization: Theory and Applications*, vol. 33, 2017.

[25] A. Gibali, G. T. Herman, and C. Schnörr, Eds., *Superiorization versus Constrained Optimization: Analysis and Applications*, vol. 2, 2020.

[26] D. Butnariu, R. Davidi, G. T. Herman, and I. G. Kazantsev, "Stable convergence behavior under summable perturbations of a class of projection methods for convex feasibility and optimization problems," *IEEE Journal of Selected Topics in Signal Processing*, vol. 1, pp. 540–547, 2007.

[27] D. Butnariu, S. Reich, and A. J. Zaslavski, "Convergence to fixed points of inexact orbits of Bregman monotone and of nonexpansive operators in Banach spaces," in *Fixed Point Theory and its Applications, Conference Proceedings, Guanajuato, Mexico, 2005*, H. F. Nathansky, B. G. de Buen, K. Goebel, W. A. Kirk, and B. Sims, Eds. Yokahama Publishers, Yokahama, Japan, 2006, pp. 11–32.

[28] ——, "Stable convergence theorems for infinite products and powers of nonexpansive mappings," *Numerical Functional Analysis and Optimization*, vol. 29, pp. 304–323, 2008.

[29] R. Davidi, "Algorithms for Superiorization and their Applications to Image Reconstruction," Ph.D. dissertation, Department of Computer Science, The City University of New York, NY, USA, 2010. [Online]. Available: http://gradworks.umi.com/34/26/3426727.html

[30] Y. Censor, H. Heaton, and R. Schulte, "Derivative-free superiorization with component-wise perturbations," *Numerical Algorithms*, vol. 80, pp. 1219–1240, 2019.

[31] H. A. Gay and A. Niemierko, "A free program for calculating EUD-based NTCP and TCP in external beam radiotherapy," *Physica Medica*, vol. 23, pp. 115–125, 2007.

[32] H. Nystrom, M. F. Jensen, and P. W. Nystrom, "Treatment planning for proton therapy: what is needed in the next 10 years?" *The British Journal of Radiology*, vol. 93, p. 1107, 2020.

[33] Y. Censor, E. Garduño, E. S. Helou, and G. T. Herman, "Derivative-free superiorization: Principle and algorithm," *Numerical Algorithms*, vol. 88, pp. 227–248, 2021.

[34] R. F. Hurley, R. W. Schulte, V. A. Bashkirov, A. J. Wroe, A. Ghebremedhin, H. F.-W. Sadrozinski, V. Rykalin, G. Coutrakon, P. Koss, and B. Patyal, "Water-equivalent path length calibration of a prototype proton CT scanner," *Medical Physics*, vol. 39, pp. 2438–2446, 2012.

[35] R. W. Schulte, S. N. Penfold, J. Tafas, and K. E. Schubert, "A maximum likelihood proton path formalism for application in proton computed tomography," *Medical Physics*, vol. 35, pp. 4849–4856, 2008.

[36] S. N. Penfold, R. W. Schulte, Y. Censor, and A. B. Rosenfeld, "Total variation superiorization schemes in proton computed tomography image reconstruction," *Medical Physics*, vol. 37, pp. 5887–5895, 2010.

[37] Y. Censor, T. Elfving, G. T. Herman, and T. Nikazad, "On diagonally-relaxed orthogonal projection methods," *SIAM Journal on Scientific Computing*, vol. 30, pp. 473–504, 2008.

[38] B. Schultze, Y. Censor, P. Karbasi, K. E. Schubert, and R. W. Schulte, "An improved method of total variation superiorization applied to reconstruction in proton computed tomography," *IEEE Transactions on Medical Imaging*, vol. 39, pp. 294–307, 2020.

[39] G. H. Golub and C. F. Van Loan, *Matrix Computations*, 3rd ed. The Johns Hopkins University Press, Baltimore, MD, USA, 1996.

[40] S. Chandrasekaran, G. H. Golub, M. Gu, and A. H. Sayed, "Parameter estimation in the presence of bounded data uncertainties," *SIAM Journal on Matrix Analysis and Applications*, vol. 19, pp. 235–252, 1998.

[41] G. A. Watson, "Data fitting problems with bounded uncertainties in the data," *SIAM Journal on Matrix Analysis and Applications*, vol. 22, pp. 1274–1293, 2001.

[42] S. Chandrasekaran, G. H. Golub, M. Gu, and A. H. Sayed, "An efficient algorithm for a bounded errors-in-variables model," *SIAM Journal on Matrix Analysis and Applications*, vol. 20, pp. 839–859, 1999.

[43] S. Chandrasekaran, M. Gu, A. H. Sayed, and K. E. Schubert, "The degenerate bounded errors-in-variables model," *SIAM Journal on Matrix Analysis and Applications*, vol. 23, pp. 138–166, 2001.

[44] P. Karbasi, K. E. Schubert, B. Schultze, V. Bashkirov, R. P. Johnson, and R. W. Schulte, "Robust iterative methods: Convergence and applications to proton computed tomography," *AIP Conference Proceedings*, vol. 2160, 050008, 2019. [Online]. Available: https://doi.org/10.1063/1.5127700.

[45] D. Thomas, J. Lamb, B. White, S. Jani, S. Gaudio, P. Lee, D. Ruan, M. McNitt-Gray, and D. Low, "A novel fast helical 4D-CT acquisition technique to generate low-noise sorting artifact-free images at user-selected breathing phases," *International journal of radiation oncology, biology, physics*, vol. 89, pp. 191–198, 2014.

[46] B. Schultze, P. Karbasi, C. Sarosiek, G. Coutrakon, C. E. Ordoñez, N. T. Karonis, K. L. Duffin, V. A. Bashkirov, R. P. Johnson, K. E. Schubert, and R. W. Schulte, "Particle-tracking proton computed tomography—data acquisition, preprocessing, and preconditioning," *IEEE Access*, vol. 9, pp. 25 946–25 958, 2021.

[47] F. P. Preparata and M. I. Shamos, *Computational Geometry: An Introduction*. Springer Science & Business Media, 2012.

[48] M. de Berg, O. Cheong, M. van Kreveld, and M. Overmars, *Computational Geometry: Algorithms and Applications*, 3rd ed. Springer-Verlag, TELOS, Santa Clara, CA, USA, 2008.

[49] D. A. Low, P. J. Parikh, W. Lu, J. F. Dempsey, S. H. Wahab, J. P. Hubenschmidt, M. M. Nystrom, M. Handoko, and J. D. Bradley, "Novel breathing motion model for radiotherapy," *International Journal of Radiation Oncology, Biology, Physics*, vol. 63, pp. 921–929, 2005.

[50] D. A. Low, B. M. White, P. P. Lee, D. H. Thomas, S. Gaudio, S. S. Jani, X. Wu, and J. M. Lamb, "A novel CT acquisition and analysis technique for breathing motion modeling," *Physics in Medicine and Biology*, vol. 58, pp. L31–L36, 2013.

[51] M. Guo, G. Chee, D. O'Connell, S. Dhou, J. Fu, K. Singhrao, D. Ionascu, D. Ruan, P. Lee, D. A. Low, J. Zhao, and J. H. Lewis, "Reconstruction of a high-quality volumetric image and a respiratory motion model from patient CBCT projections," *Medical Physics*, vol. 46, pp. 3627–3639, 2019.

[52] G. Chee, D. O'Connell, Y. M. Yang, K. Singhrao, D. A. Low, and J. H. Lewis, "McSART: an iterative model-based, motion-compensated SART algorithm for CBCT reconstruction," *Physics in Medicine and Biology*, vol. 64, p. 095013, 2019.

[53] J. Eom, X. G. Xu, S. De, and C. Shi, "Predictive modeling of lung motion over the entire respiratory cycle using measured pressure-volume data, 4DCT images, and finite-element analysis," *Medical Physics*, vol. 37, pp. 4389–4400, 2010.

[54] J. Ehrhardt, R. Werner, A. Schmidt-Richberg, and H. Handels, "Statistical modeling of 4D respiratory lung motion using diffeomorphic image registration," *IEEE Transactions on Medical Imaging*, vol. 30, pp. 251–265, 2011.

[55] Y. Zhang, J. Yang, L. Zhang, L. E. Court, P. A. Balter, and L. Dong, "Modeling respiratory motion for reducing motion artifacts in 4D CT images," *Medical Physics*, vol. 40, p. 041716 (13pp), 2013.

[56] M. Buhmann, *Radial Basis Functions: Theory and Implementations*. Cambridge University Press, 2003.

[57] R. M. Lewitt, "Alternatives to voxels for image representation in iterative reconstruction algorithms," *Physics in Medicine and Biology*, vol. 37, pp. 705–716, 1992.

[58] ——, "Multidimensional digital image representations using generalized Kaiser–Bessel window functions," *Journal of the Optical Society of America A*, vol. 7, pp. 1834–1846, 1990.

[59] G. T. Herman, "Basis Functions in Image Reconstruction From Projections: A Tutorial Introduction," *Sensing and Imaging*, vol. 16, pp. 1–21, 2015.

[60] S. Matej and R. Lewitt, "Efficient 3D grids for image reconstruction using spherically symmetric volume elements," *IEEE Transactions on Nuclear Science*, vol. 42, pp. 1361–1370, 1995.

[61] ——, "Practical considerations for 3-D image reconstruction using spherically symmetric volume elements," *IEEE Transactions on Medical Imaging*, vol. 15, pp. 68–78, 1996.

[62] H. Heaton, C. Ordonez, Y. Censor, and R. Schulte, "Implementation of blob basis functions in proton CT reconstruction," *Poster presented at the Joint Mathematics Meetings (JMM) of the*

MAA and the AMS, Meeting #1116, January 6-9, 2016, Seattle, WA, USA. http://math.haifa.ac.il/yair/webpage-after-200915/JMM-Blob-Poster-2016.pdf.

[63] Y. Benkarroum, G. T. Herman, and S. W. Rowland, "Blob parameter selection for image representation," *Journal of the Optical Society of America A*, vol. 32, pp. 1898–1915, 2015.

[64] S. Penfold, R. Zalas, M. Casiraghi, M. Brooke, Y. Censor, and R. Schulte, "Sparsity constrained split feasibility for dose-volume constraints in inverse planning of intensity-modulated photon or proton therapy," *Physics in Medicine and Biology*, vol. 62, pp. 3599–3618, 2017.

[65] S. Penfold, M. Casiraghi, T. Dou, R. Schulte, and Y. Censor, "A feasibility-seeking algorithm applied to planning of intensity modulated proton therapy: A proof of principle study," *Medical Physics*, vol. 42, p. 3338, 2015.

[66] R. Hesse, D. R. Luke, and P. Neumann, "Alternating projections and Douglas-Rachford for sparse affine feasibility," *IEEE Transactions on Signal Processing*, vol. 62, pp. 4868–4881, 2014.

[67] Y. Censor and T. Elfving, "A multiprojection algorithm using Bregman projections in a product space," *Numerical Algorithms*, vol. 8, pp. 221–239, 1994.

[68] Y. Censor, T. Elfving, N. Kopf, and T. Bortfeld, "The multiple-sets split feasibility problem and its applications for inverse problems," *Inverse Problems*, vol. 21, pp. 2071–2084, 2005.

[69] Y. Censor, A. Gibali, and S. Reich, "Algorithms for the split variational inequality problem," *Numerical Algorithms*, vol. 59, pp. 301–323, 2012.

[70] M. Brooke, Y. Censor, and A. Gibali, "Dynamic string-averaging CQ-methods for the split feasibility problem with percentage violation constraints arising in radiation therapy treatment planning," *International Transactions in Operational Research*, 2020, https://onlinelibrary.wiley.com/doi/full/10.1111/itor.12929.

[71] C. Byrne, "Iterative oblique projection onto convex sets and the split feasibility problem," *Inverse Problems*, vol. 18, pp. 441–453, 2002.

[72] Y. Censor, "An automatic relaxation method for solving interval linear inequalities," *Journal of Mathematical Analysis and Applications*, vol. 106, pp. 19–25, 1985.

[73] K. Maass, M. Kim, and A. Aravkin, "A nonconvex optimization approach to IMRT planning with dose-volume constraint," 2020, preprint. https://arxiv.org/pdf/1907.10712.pdf.

[74] V. A. Bashkirov, R. P. Johnson, H. F.-W. Sadrozinski, and R. W. Schulte, "Development of proton computed tomography detectors for applications in hadron therapy," *Nuclear Instruments & Methods in Physics Research Section A: Accelerators, Spectrometers, Detectors and Associated Equipment*, vol. 809, pp. 120–129, 2016.

[75] M. Witt, B. Schultze, R. Schulte, K. Schubert, and E. Gomez, "A proton simulator for testing implementations of proton CT reconstruction algorithms on GPGPU clusters," in *Proceedings of the IEEE Nuclear Science Symposium & Medical Imaging Conference (NSS/MIC) 2012, Anaheim, CA, USA*, 2012, pp. 4329–4334.

[76] B. Schultze, P. Karbasi, V. Giacometti, T. Plautz, K. E. Schubert, and R. W. Schulte, "Reconstructing highly accurate relative stopping powers in proton computed tomography," in *Proceedings of the IEEE Nuclear Science Symposium & Medical Imaging Conference (NSS/MIC), San Diego, CA, USA, 2015*, 2015, pp. 1–3, doi:10.1109/NSSMIC.2015.7582218.

[77] R. P. Johnson, V. A. Bashkirov, G. Coutrakon, V. Giacometti, P. Karbasi, N. T. Karonis, C. Ordoñez, M. Pankuch, H. F.-W. Sadrozinski, K. E. Schubert, and R. W. Schulte, "Results from a prototype proton-CT head scanner," *Physics Procedia*, vol. 90, pp. 209–214, 2017.

[78] P. Karbasi, R. Cai, B. Schultze, H. Nguyen, J. Reed, P. Hall, V. Giacometti, V. Bashkirov, R. Johnson, N. Karonis, J. Olafsen, C. Ordonez, K. E. Schubert, and R. W. Schulte, "A highly accelerated parallel multi-GPU based reconstruction algorithm for generating accurate relative stopping powers," in *2017 IEEE Nuclear Science Symposium and Medical Imaging Conference (NSS/MIC), Atlanta, GA, USA*, 2017, pp. 1–4, doi:10.1109/NSSMIC.2017.8532871.

[79] R. P. Johnson, V. A. Bashkirov, L. DeWitt, V. Giacometti, R. F. Hurley, P. Piersimoni, T. E. Plautz, H. F.-W. Sadrozinski, K. E. Schubert, R. W. Schulte, B. E. Schultze, and A. Zatserklyaniy, "A fast experimental scanner for proton CT: Technical performance and first experience with phantom scans," *IEEE Transactions on Nuclear Science*, vol. 63, pp. 52–60, 2016.

[80] P. Karbasi, "Robust and efficient methods for proton computed tomography," Ph.D. dissertation, Electrical and Computer Engineering, Baylor University, Baylor, TX, USA, 2018.

[81] S. Agostinelli, J. Allison, K. Amako, J. Apostolakis, H. Araujo, P. Arce, M. Asai, D. Axen, S. Banerjee, G. Barrand, F. Behner, L. Bellagamba, J. Boudreau, L. Broglia, A. Bruneng, H. Burkhardt, S. Chauvie, J. Chuma, R. Chytracek, and G. Coopermana, "Geant4 - a simulation toolkit," *Nuclear Instruments and Methods in Physics Research, Section A: Accelerators, Spectrometers, Detectors and Associated Equipment*, vol. 506, pp. 250–303, https://doi.org/10.1016/S0168-9002(03)01368-8.

[82] V. Giacometti, "Modelling and Improvement of Proton Computed Tomography," Ph.D. dissertation, School of Physics, University of Wollongong, Australia, 2016, https://ro.uow.edu.au/theses/4903.

[83] J. Perl, J. Shin, J. Schümann, B. Faddegon, and H. Paganetti, "TOPAS: An innovative proton Monte Carlo platform for research and clinical applications," *Medical Physics*, vol. 39, pp. 6818–6837, 2012.

[84] P. Piersimoni, J. Ramos-Méndez, T. Geoghegan, V. A. Bashkirov, R. W. Schulte, and B. A. Faddegon, "The effect of beam purity and scanner complexity on proton CT accuracy," *Medical Physics*, vol. 44, pp. 284–298, 2017.

[85] P. Piersimoni, B. A. Faddegon, J. Ramos-Méndez, R. W. Schulte, L. Volz, and J. Seco, "Helium CT: Monte Carlo simulation results for an ideal source and detector with comparison to proton CT," *Medical Physics*, vol. 45, pp. 3264–3274, 2018.

[86] V. Giacometti, S. Guatelli, M. Bazalova-Carter, A. B. Rosenfeld, and R. W. Schulte, "Development of a high resolution voxelised head phantom for medical physics applications," *Physica Medica*, vol. 33, pp. 182–188, 2017.

[87] S. Guatelli and S. Incerti, "Monte Carlo simulations for medical physics: From fundamental physics to cancer treatment," *Physica Medica*, vol. 33, pp. 179–181, 2017.

[88] V. Giacometti, V. A. Bashkirov, P. Piersimoni, S. Guatelli, T. E. Plautz, H. F.-W. Sadrozinski, R. P. Johnson, A. Zatserklyaniy, T. Tessonnier, K. Parodi, A. B. Rosenfeld, and R. W. Schulte, "Software platform for simulation of a prototype proton CT scanner," *Medical Physics*, vol. 44, pp. 1002–1016, 2017.

[89] R. Schulte, K. Schubert, and Y. Censor, "Computational tools for real-time adaptive particle therapy," 2013, this is a research grant from the United States-Israel Binational Science Foundation (BSF), Grant Number 2013003, 10/2014-9/2019.

[90] R. Schulte and Y. Censor, "Intensity modulation and proton computed tomography in proton radiation therapy planning," 2009, this is a research grant from the United States-Israel Binational Science Foundation (BSF), Grant Number 2009012, 10/2010-9/2013.

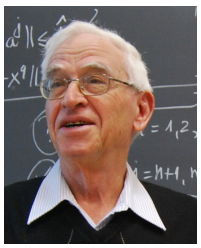

Yair Censor received his B.Sc., M.Sc. and D.Sc. degrees in mathematics from the Technion-Israel Institute of Technology in Haifa in 1967, 1969 and 1975, respectively. From 1977 to 1979, he was Research Assistant Professor of Computer Science at the State University of New York (SUNY) at Buffalo, NY, USA, and Research Associate with the Medical Image Processing Group (MIPG) there.

In 1979, Dr. Censor joined the Department of Mathematics at the University of Haifa in Israel, where he has been Full Professor since 1989 and became Professor Emeritus in 2012. He was a visiting professor at the University of Pennsylvania in Philadelphia; in Linköing University in Sweden; in the Instituto de Matematica Pura e Aplicada in Rio de Janeiro, Brazil; in the Beijing International Center of Mathematics at the Peking University in Beijing, China; and in the Graduate Center of the City University of New York.

Dr. Censor works in computational mathematics, where his interests include optimization theory, inverse problems, optimization techniques in image reconstruction from projections, and in intensity-modulated radiation therapy (IMRT). Dr. Censor has published over 160 research articles in refereed scientific journals, conference proceedings and as book chapters. He co-authored with S.A. Zenios the book: Parallel Optimization: Theory, Algorithms, and Applications, Oxford University Press, New York, 1997. For this book he received, together with Professor Zenios, the 1999 ICS (INFORMS Computing Society) Prize for research excellence in the interface between operations research and computer science. Dr. Censor served as Associate Editor for the journal IEEE Transactions on Medical Imaging from 1992 to 2004.

Keith E. Schubert received his B.S. degree in general engineering from the University of Redlands in 1991, his M.S. in electrical engineering from UCLA in 1992. After working for a few years, he earned his Ph.D. in electrical and computer engineering from UCSB in 2003 for work on computational methods of uncertain systems and robustness in estimation and control.

From 1992-1996 he worked for Northrop-Grumman as a design engineer, and since 1996 he has worked as a consulting engineer for various companies. In 2000, he took a visiting faculty position at the University of Redlands in mathematics and computer science for two years, then was hired as an assistant professor in 2002 at CSU San Bernardino, where he became an associate professor in 2006, then a full professor in 2010. At CSUSB he was the lead on starting their first engineering program and was part of the team that started the Bioinformatics program. In 2013, he joined Baylor University in Waco, Tx, where he is currently a full professor in electrical and computer engineering. His research is in devices and computational methods for robust imaging particularly for biomedical applications.

Dr. Schubert has several patents and served as Principal Investigator on the NIH R01 grant to develop proton CT for biomedical applications from 2011-2016 and as part of the research team for a planning grant (P20) for the development of ion therapy research in the United States from 2015-2017. In 2013, Dr. Schubert was one of the team leaders of a National Geographic research expedition to Cueva de Villa Luz in Mexico, where he studied patterned biological grows in the sulfuric acid caves, which was featured in the July 2014 cover article of National Geographic Magazine.

Reinhard W. Schulte (M'12) received his diploma degree (M.S. equivalent) in physics (Diplom Physiker, Dipl. Phys.) from the University of Dortmund, Germany, in 1978, and his doctorate in medicine (Doctor of Medicine, Dr. med.) from the University of Cologne, Germany, in 1986. He completed his residency in radiology and radiation oncology at Hannover Medical School in 1989.

He was a postdoctoral fellow at the first hospital-based proton therapy center at Loma Linda University Medical Center (LLUMC) in California from 1990-1994. In 1994 he accepted a clinical research position at LLUMC. In 1996, he became an Assistant Clinical Professor in the School of Medicine and the Department of Radiation Medicine at LLUMC, In 2007, he was promoted to Associate Professor, and since 2013, he has been a Full Professor at Loma Linda University, now in the Department of Basic Sciences, Division of Biomedical Engineering Sciences. He has been successful in developing novel instrumentation and algorithmic approaches for proton therapy. His current research interests include the clinical development of proton CT and nanodosimetry to improve proton and ion therapy. He is an Associate Editor of the journal Medical Physics and holds several patents.

Prof. Schulte was awarded a habilitation fellowship by the German Research Foundation (Deutsche Forschungsgemeinschaft, DFG) from 1989-1991. He is a member of the American Society of Radiation Oncology (ASTRO), the European Society of Therapeutic Radiation Oncology (ESTRO), the American Association of Physicists in Medicine (AAPM), the German Society for Boron Neutron Capture Therapy, and the Radiation Research Society. He was awarded the ESTRO Calergo Award in 1990. Prof. Schulte has served as Principal Investigator on several NIH grants, including an R01 grant to develop proton CT for biomedical applications from 2011-2016 and a planning grant (P20) for the development of ion therapy research in the United States from 2015-2017.